Physica Medica 66 (2019) 29–35

Contents lists available at ScienceDirect

Physica Medica

journal homepage: www.elsevier.com/locate/ejmp

Original paper

Estimation of radiation shielding ability in electron therapy and brachytherapy with real time variable shape tungsten rubber

Hajime Monzen[a,*], Mikoto Tamura[a], Kenta Kijima[a], Masakazu Otsuka[a,b], Kenji Matsumoto[a,b], Kazuki Wakabayashi[a], Min-Geon Choi[a,c], Do-Kun Yoon[c], Hiroshi Doi[d], Hironori Akiyama[e], Yasumasa Nishimura[d]

[a] Department of Medical Physics, Graduate School of Medical Sciences, Kindai University, Osaka-Sayama, Osaka 589-8511, Japan
[b] Department of Central Radiology, Kindai University Hospital, Osaka-Sayama, Osaka 589-8511, Japan
[c] Department of Biomedical Engineering and Research Institute of Biomedical Engineering, College of Medicine, Catholic University of Korea, Seoul 06591, South Korea
[d] Department of Radiation Oncology, Faculty of Medicine, Kindai University, 377-2 Ohno-higashi, Osaka-Sayama, Osaka 589-8511, Japan
[e] Department of Oral Radiology, Osaka Dental University, 1-5-17 Otemae Chuo-ku, Osaka 540-0008, Japan

ARTICLE INFO

Keywords:
Real time variable shape
Tungsten rubber
Radiation protection
Electron beam
Brachytherapy

ABSTRACT

Purpose: To clarify the physical characteristics of a newly developed real time variable shape rubber containing tungsten (STR) with changes in heat and estimate its shielding abilities against electron beams and γ-rays from ^{192}Ir.

Methods: Dynamic mechanical analysis for the STR (density = 7.3 g/cm^3) was conducted at a frequency of 1.0 Hz in the temperature range of −60 °C to 60 °C. We evaluated tanδ, defined as the ratio (E″/E′) between the storage modulus (E′) and loss modulus (E″). The transmission rates were measured against 6- and 12-MeV electron beams and the percentage depth dose and lateral dose profile were compared with low-melting alloy (LMA). For the shielding rate of ^{192}Ir against γ-rays, measurement data and Monte Carlo simulation data were obtained with STR thickness ranging from 1.0 mm to 16.0 mm.

Results: At 36 °C, the tanδ value was 0.520, while at 60 °C, this value was 1.016. For 6- and 12-MeV electron beams, the transmission rates decreased with increasing STR thickness and reached plateaus at approximately 1.0% and 4.0% with STR thickness of > 7.0 and > 12.0 mm, respectively. The dose distributions were almost equal to those for LMA. Against γ-rays, the thickness of STR that obtained a 50% attenuation rate for ^{192}Ir was 5.804 mm. The Monte Carlo calculation results were 2.6% higher on average than the measurement results.

Conclusion: The STR can be changed shape in real time at 60 °C and maintains its shape at body temperatures. It has adequate shielding abilities against megavoltage electron beams and γ-rays from ^{192}Ir.

1. Introduction

Lead has been employed for radiation protection in the clinical setting for many years. Its uses include shielding for occupational protection in the medical and industrial fields as well as during electron beam radiotherapy. The shortcomings of shielding materials made of lead or lead equivalent include inflexibility and toxicity [1,2]. There is therefore a strong demand for lead-free product development in healthcare and industrial applications. For the production of lead-free radiation-shielding materials, we have developed a real time variable shape rubber containing tungsten (STR) (Hayakawa Rubber Co., Ltd. Hiroshima, Japan). The tungsten belongs to the group of refractory metals with a molecular weight of 183.85 and the highest melting point (3410 °C) of all elements except carbon, clinical follow-up in patients after tungsten coil implantation did not demonstrate any evidence for toxicity [3]. In previous studies, we reported on the electron beam, γ-ray, and X-ray shielding abilities of Tungsten functional paper (TFP) [4–10] and Tungsten-containing rubber (TCR) [11–13]. Both materials were shown to be particularly promising for radiation protection, even though they are lead-free. The STR has several benefits to compare with TFP and TCR, such as easy to shape in real time at approximately 60 °C and maintains its shape at room temperature and body temperature. In addition, the contained tungsten can be gathered for reuse by heat treatment.

In general, collimators for electron therapy made from lead or a low-melting point alloy (LMA) are widely used in clinical site [14–16].

* Corresponding author.
E-mail address: hmon@med.kindai.ac.jp (H. Monzen).

https://doi.org/10.1016/j.ejmp.2019.09.233
Received 6 August 2019; Received in revised form 28 August 2019; Accepted 14 September 2019
Available online 21 September 2019

These lead and LMA shields have problems such as limiting radiation to the appropriate area by shaping the irradiation field, being difficult to process and taking a long time to shape, harmful effects on the environment, and possible toxicity to the human body [17]. It is problematic that patients who have developed a keloid on their earlobe or abdomen may need to undergo electron therapy as soon as possible after excision. Leeuwen et al. showed that in an external radiation group, the rate of recurrence of keloid scars decreased when radiation was applied within 7 h, compared with 24 h or longer after excision [18]. It is very difficult to perform electron therapy immediately after excision using lead or LMA. Additionally, lead or LMA is difficult to adapt to the movements of the target in terms of respiration and patient motion, which can require the irradiation field to have a large margin. The STR will be able to solve all of these problems and may have the potential to open a new era in this field.

Brachytherapy for oral cancers is another current application of lead use in clinical radiotherapy [19,20]. High-dose-rate (HDR) interstitial brachytherapy is a considerable treatment option for various cancers including uterine cervical cancer, prostate cancer, and oral cancers [19]. HDR brachytherapy a definitive treatment option for cancer of the oral cavity because it can provide an excellent loco-regional control rate and also has the advantage of preserving the shape and functions of the oral cavity, including the tongue [20]. However, brachytherapy for oral cancer could cause severe toxicities in the normal mucosa and mandible with increased doses of radiation exposure [21]. With the aim of reducing these toxicities, several devices have been developed to assist with brachytherapy for oral cancers [22,23]. Murakami et al. reported that spacers using embedded metals could reduce irradiation exposure [23]. However, mandible lead shields might produce various side effects of lead in the oral cavity. Moreover, potential secondary scatter radiation can be emitted from the surface of a lead-only spacer [23]. Therefore, STR could be an alternative material with the potential to overcome the problems with lead materials in brachytherapy for oral tongue cancer using oral devices.

The purpose of this study is to clarify the thermal characteristics and the dynamic viscoelasticity of the STR and to investigate the feasibility of an application of the STR to clinical radiation therapy through verification of its shielding ability against electron beams and γ-rays from ^{192}Ir. For physical characteristic analysis, the dynamic viscoelasticity of the STR was evaluated in temperature range of −60 °C to 60 °C. The transmission rates in various thicknesses of STRs for megavoltage electron beams were measured and compared with those of LMA. For the ^{192}Ir shielding rate against γ-rays, we compared measurement data and Monte Carlo n-particle extended (MCNPX, Ver.2.6.0, LANL, Los Alamos, NM, USA) simulation code data with mathematical calculations based on a computing process [24]. The dosimetric characteristics with both radiation types and their possible clinical applications are discussed.

2. Materials and methods

2.1. STR characteristics

The STR is a rubber material with no cross-linked polymerization, and it is a real time variable shaped material. Therefore, it is possible to change shape by hand at temperatures of approximately 60 °C and maintains its shape at room temperature (Fig. 1).

The STRs with density of 7.3 g/cm^3 were provided by Hayakawa Rubber Co. The elemental ratio (wt%) in STR was C: 5.5%, H: 0.9%, O: 1.4%, and W: 92.2%. To assess its thermal characteristics, the dynamic viscoelasticity of the STR was evaluated with a dynamic mechanical thermal analysis machine [25] (DMS6100; Hitachi High-Tech Science Co., Tokyo, Japan). The dynamic mechanical analysis for the STR with dimensions of 5.0 (W) × 45.0 (L) × 2.0 (T) mm^3 was conducted at a frequency of 1.0 Hz [26,27] and an amplitude of 10 μm in temperature range from −60 °C to 60 °C with a heating rate of 2 °C/min. Then, the storage modulus (E′) as elasticity and loss modulus (E″) as viscosity were obtained, and the ratio of the moduli (E″/E′, defined as tanδ) was evaluated under each temperature. A high tanδ value means high viscosity, while a low tanδ means high elasticity (i.e. tanδ = 0 means a perfectly elastic solid).

2.2. Shielding ability and dosimetric characteristics for megavoltage electron beams

The irradiated fields of electron beams were shaped using the LMA and STR. The thickness of the LMA set on the electron applicator was 1.4 cm, as with conventional electron therapy, while the thicknesses of the STR was varied from 1.0 to 12.0 mm at room temperature and from 2.0 to 16.0 mm for 6- and 12-MeV electron beams, respectively. The electron applicator size was 10 × 10 cm^2, and 200 monitor units were irradiated.

First, for evaluation of the STR's shielding ability, the transmission was measured by geometry, as shown in Fig. 2a. The STR was set on a solid water phantom (GAMMEX, Wisconsin, USA), and the doses for each STR thickness at depths of 0, 0.5, and 1.5 cm were measured with a plate parallel ionization chamber (PPIC) (Markus Ion Chamber; PTW, Freiburg, Germany) three times [11]. Second, for evaluation of the STR's dosimetric characteristics, 3.0 cm along the X-axis was blocked with the LMA or STR, as shown in Fig. 2b [11]. The percentage depth dose (PDD) along the beam axis and the lateral dose profiles were measured using a solid water phantom and Gafchromic EBT3 film (ISP, Wayne, NJ, USA). The film was set up parallel to the beam axis for PDD, and lateral dose profile measurements were taken. For surface lateral dose profile measurement, the film was set up perpendicular to the beam axis at the surface. The depths with maximum dose (d_{max}), 90% dose (d_{90}), and 80% dose (d_{80}) were obtained from the PDD curves. The lateral dose profiles were normalized by the values at the center, and the maximum dose within the irradiated field at the surface and the penumbra (as the width of the off-axis distance from 80% to 20% dose levels, $P_{80\text{-}20}$) were evaluated at the surface, d_{max}, d_{90}, and d_{80}.

2.2.1. Shielding rates of STR against γ-rays from ^{192}Ir

The shielding rates of STRs for an ^{192}Ir (Activity: 199.4 GBq) microSelectron HDR source (Elekta AB, Stockholm, Sweden) were measured at room temperature with the PPIC and solid water (GAMMEX, Wisconsin, USA), as shown in Fig. 3. The STR sheet of size 10.0 × 10.0 cm^2 was set on the solid water phantom, and the radiation source was 2.0 cm above the surface of the phantom. The PPIC was set on the phantom, and measurements were performed with increased STR thickness. The irradiation time was 30 sec. For measurement accuracy, the doses with irradiation time 60 sec were also measured and subtracted from the doses with 30-sec irradiation times. Then, the transmission rates were measured while changing the STR thickness from 0.0 (no shield) to 16.0 mm at an interval of 1.0 mm.

2.2.2. Monte Carlo calculation of dosimetric properties with ^{192}Ir

To validate the accuracy of the shielding rate measurement of the STR, Monte Carlo simulation was performed. The simulation tool was Monte Carlo n-particle extended (MCNPX, Ver: 2.6.0, LANL, Los Alamos National Laboratory, USA). For the simulation's geometric setup, both the water phantom (20 cm (X-axis) × 20 cm (Y-axis) × 10 cm (Z-axis)) and the STR were defined according to the actual experimental setup, as shown in Fig. 3. The energy of γ-rays from the ^{192}Ir source in the simulation was set as 317 keV (83%), 468 keV (48%), and 604 keV (8%) using both the source information and probability cards, which contain integers in MCNPX. The cutoff energies of photons and electrons were both 1.0 eV. Comparison of the transmission rate between measurement and calculation was performed for each STR thickness.

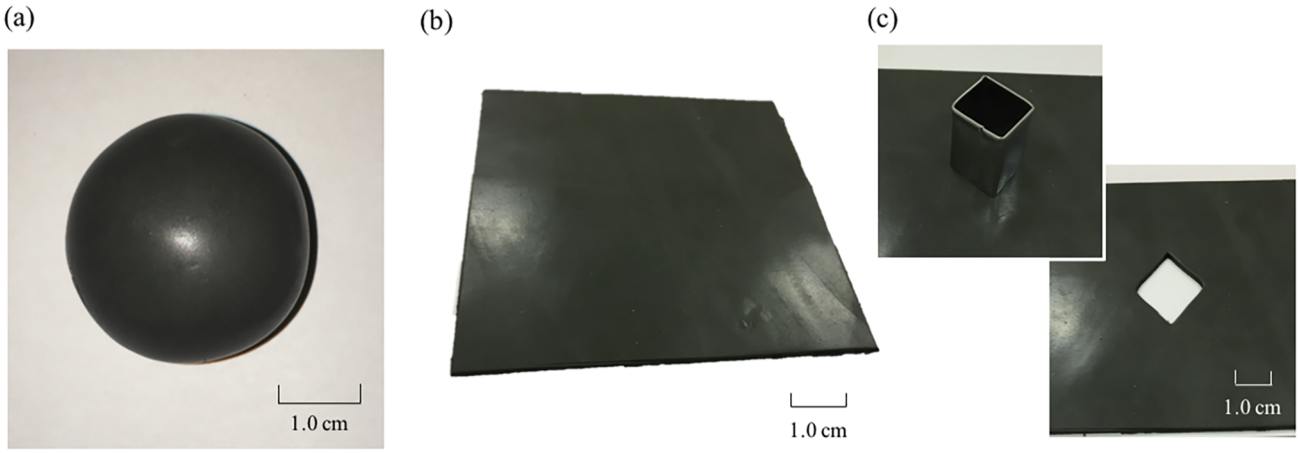

Fig. 1. A real time variable shape rubber containing tungsten (STR) can be changed shape by heat to (a) ball type and (b) sheet type and (c) easy to process (e.g. cutting out).

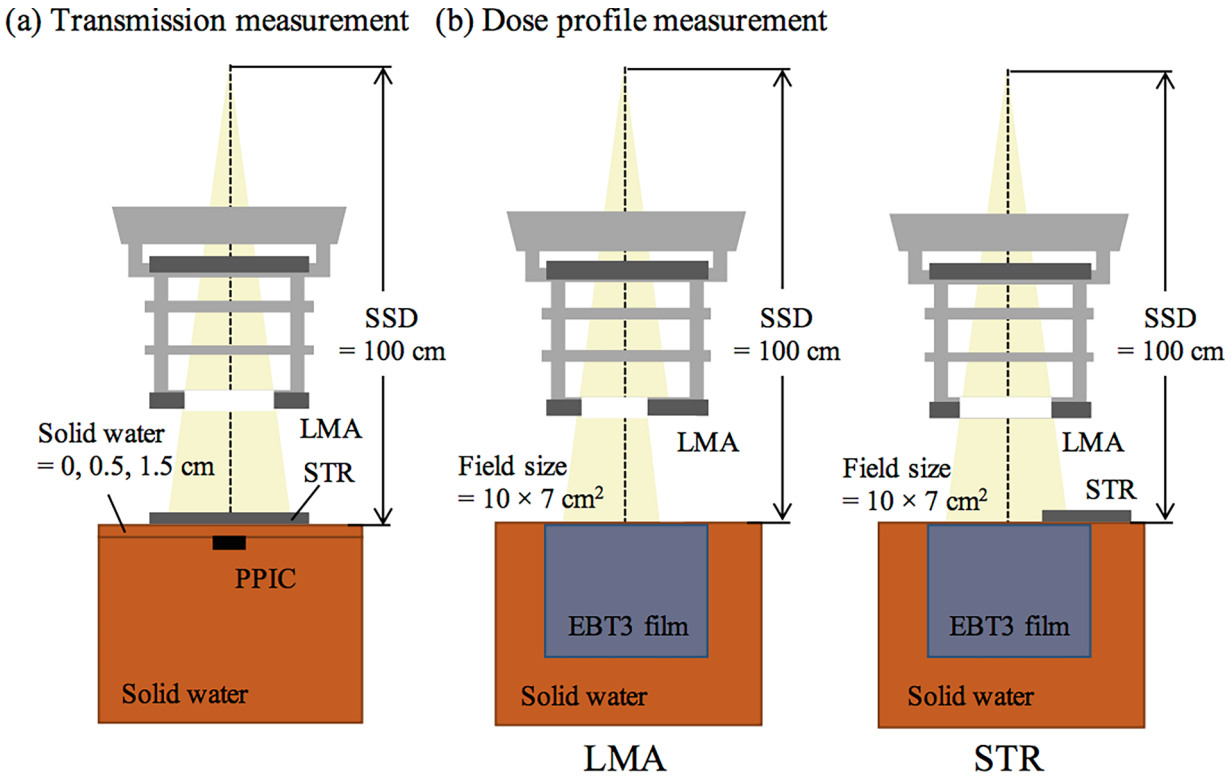

Fig. 2. Schematics of geometry for measurement of (a) transmission and (b) dose profiles.

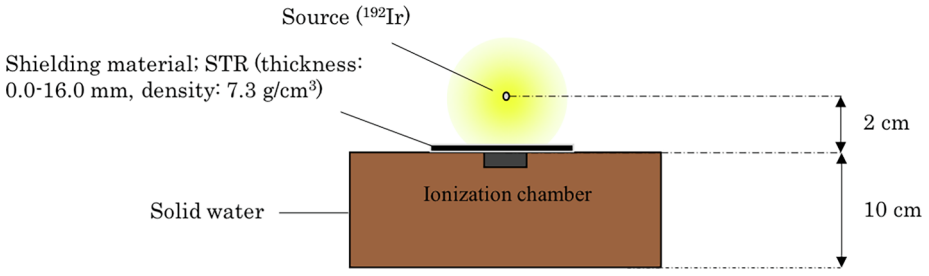

Fig. 3. Drawing of geometry of setup used to determine shielding rate against γ-rays from ^{192}Ir.

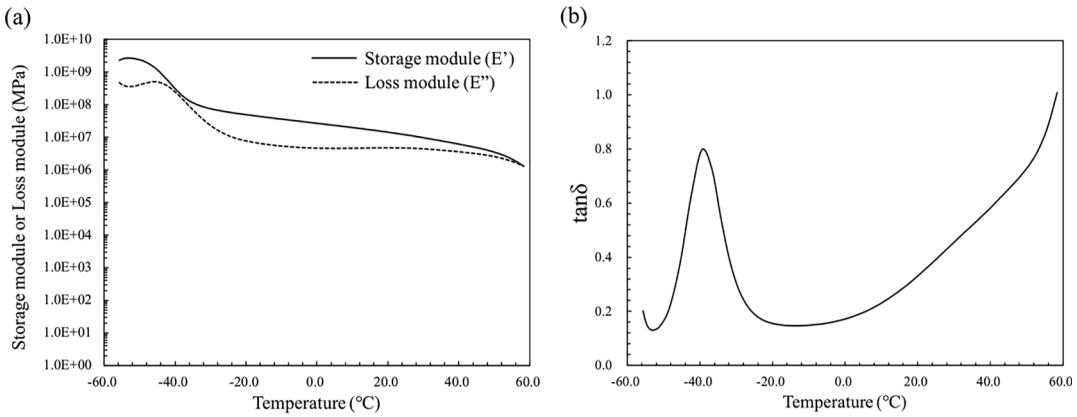

Fig. 4. Dynamic mechanical analysis results for the STRs. (a) Relationship between temperature and elasticity (E′) and viscosity (E″). (b) Relationship between temperature and tanδ = E″/E′.

3. Results

3.1. Temperature characteristics of the STR

Fig. 4 shows the temperature characteristics of the STR. Its elasticity decreased with increasing temperature, while tanδ had a peak around −38 °C due to the glass transition temperature [25]. The tanδ increased with increasing temperature in the > 0 °C range, i.e. the viscosity increased with temperature. At 36 °C, close to body temperature, the tanδ value of the STR was 0.520, while at 60 °C, this value was 1.016. The STR could be changed shape easily by hand, with a tanδ value greater than 0.600, at 40 °C. In contrast, the STR could maintain its shape (tanδ < 0.600). In this experiment, the temperature limit was 60 °C because the STR was torn off due to high viscosity at temperatures of > 60 °C.

3.2. Shielding ability and dosimetric characteristics with megavoltage electron beams

The transmission rates of the STR are shown in Table 1. For 6 and 12 MeV electron beams, the transmission rates decreased with increasing STR thickness and reached plateau values of approximately 1.0% and 4.0% at STR thickness of > 7.0 and > 12.0 mm, respectively.

Table 2 shows the dosimetric characteristics of the PDD curves in Fig. 5. For the LMA, the d_{max}, d_{90}, and d_{80} with 6 and 12 MeV beams were 12.6 and 28.6 mm, 17.2 and 39.0 mm, and 19.0 and 43.1 mm, respectively. In contrast, for STR materials of thickness 7.0 and 12.0 mm with 6 and 12 MeV beams, the d_{max}, d_{90}, and d_{80} were 13.5 and 25.9 mm, 18.4 and 36.2 mm, and 19.9 and 40.9 mm, respectively. The differences between LMA and STR with these parameters ranged from 1.0 to 3.0 mm.

Table 1
Transmission rates (%) of a real time variable shape rubber containing tungsten (STR) for each solid water thickness.

		STR thickness (mm)								
6 MeV	Depth	0	1.0	2.0	3.0	4.0	5.0	7.0	10.0	12.0
	Surface	100.0	123.9	55.4	12.9	3.0	2.3	1.5	1.3	1.2
	0.5 cm	100.0	82.2	28.7	5.2	1.8	1.7	1.4	1.1	1.0
	1.5 cm	100.0	26.8	4.0	1.5	1.4	1.3	1.2	1.0	0.9
		STR thickness (mm)								
12 MeV	Depth	0	2.0	4.0	6.0	8.0	10.0	12.0	14.0	16.0
	Surface	100.0	130.8	70.7	20.2	6.5	4.9	4.5	4.1	3.7
	0.5 cm	100.0	112.0	53.5	13.7	5.3	4.4	4.0	3.7	3.4
	1.5 cm	100.0	83.4	29.3	6.8	4.1	3.7	3.4	3.2	2.9

Table 2
Dosimetric characteristics of PDD with LMA and STR.

(a) Depth at maximum dose (d_{max}) (mm)

6 MeV	LMA	STR thickness (mm)						
		1.0	2.0	3.0	4.0	5.0	7.0	10.0
	12.6	13.0	12.3	13.5	13.0	13.3	13.5	13.5
12 MeV	LMA	STR thickness (mm)						
		2.0	4.0	6.0	8.0	10.0	12.0	14.0
	26.6	28.2	28.2	28.2	29	27.7	25.9	27.6

(b) Depth at 90% dose (d_{90}) (mm)

6 MeV	LMA	STR thickness (mm)						
		1.0	2.0	3.0	4.0	5.0	7.0	10.0
	17.2	17.3	19.2	19.6	17.6	17.8	18.4	19.5
12 MeV	LMA	STR thickness (mm)						
		2.0	4.0	6.0	8.0	10.0	12.0	14.0
	38.4	38.2	37.9	38.6	38.0	36.5	36.2	37.5

(c) Depth at 80% dose (d_{80}) (mm)

6 MeV	LMA	STR thickness (mm)						
		1.0	2.0	3.0	4.0	5.0	7.0	10.0
	19.0	19.5	19.1	20.8	19.3	20.2	19.9	20.1
12 MeV	LMA	STR thickness (mm)						
		2.0	4.0	6.0	8.0	10.0	12.0	14.0
	41.9	43.0	42.6	41.6	41.3	41.0	40.9	41.6

Table 3 shows the dosimetric characteristics of the STR with lateral dose profiles, and Fig. 6 shows the lateral dose profiles of the LMA and STR with 6 and 12 MeV electron beams. Only in the surface lateral dose profile, a high dose was observed at the edge of the irradiated field; however, the magnitude of the high dose decreased with increasing STR thickness and depth. The maximum dose at the surface was 117.0% and 126.6% for STR thickness 7.0 and 12.0 mm, respectively. The $P_{80\text{-}20}$ values of the STR were smaller than those of the LMA, although the differences in $P_{80\text{-}20}$ values decreased with increasing depth. In particular, for the 12 MeV beam, the $P_{80\text{-}20}$ values at the d_{max}, d_{90}, and d_{80} were almost equal between LMA and STR. The $P_{80\text{-}20}$ values at the surface, d_{max}, d_{90}, and d_{80} using the STR with thickness 7.0 and 12.0 mm with 6 and 12 MeV beams were 0.3 and 0.6 mm, 5.7 and 10.0 mm, 7.6 and 15.3 mm, and 8.3 and 17.5 mm, respectively, whereas

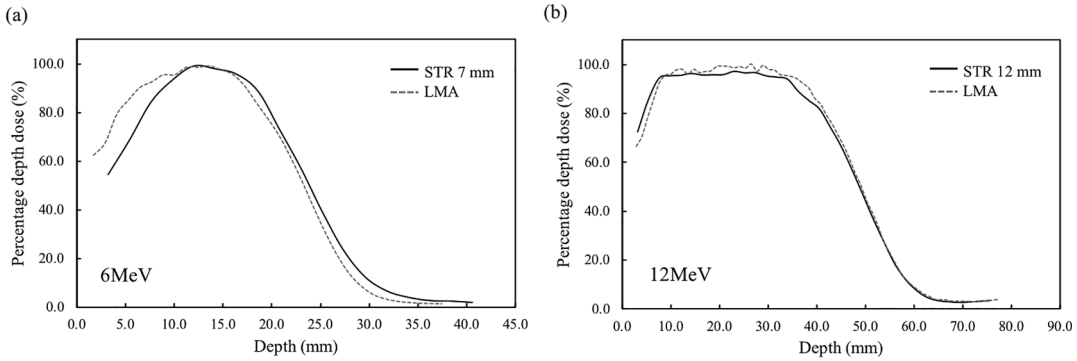

Fig. 5. Depth dose profiles (PDD) for LMA and STR with thickness of 7.0 and 12.0 mm for (a) 6 and (b) 12 MeV electron beams.

Table 3
Dosimetric characteristics of lateral dose profiles using LMA and STR.

(a) Maximum dose at surface, d_{max}, d_{90}, and d_{80} (%)

6 MeV		LMA	STR thickness (mm)						
			1.0	2.0	3.0	4.0	5.0	7.0	10.0
	Surface	106.8	150.4	136.2	122.1	115.8	126.0	117.0	118.7
	d_{max}	103.9	107.3	104.6	104.0	105.2	106.2	104.2	104.2
	d_{90}	104.8	102.6	103.5	103.1	105.3	104.2	105.2	104.4
	d_{80}	104.2	104.3	106.2	105.3	103.7	105.3	104.4	105.6
12 MeV		LMA	STR thickness (mm)						
			2.0	4.0	6.0	8.0	10.0	12.0	14.0
	Surface	107.7	157.8	151.3	126.5	122.2	130.1	126.6	125.2
	d_{max}	103.9	104.7	103.0	102.2	103.8	102.9	103.0	103.0
	d_{90}	104.2	102.4	103.7	105.8	101.8	104.0	104.1	104.1
	d_{80}	104.0	102.5	104.8	103.6	101.7	103.3	102.2	102.0

(b) $P_{80\text{-}20}$ at surface, d_{max}, d_{90}, and d_{80} (mm)

6 MeV		LMA	STR thickness (mm)						
			1.0	2.0	3.0	4.0	5.0	7.0	10.0
	Surface	5.7	–	–	0.3	0.3	0.2	0.3	0.2
	d_{max}	9.7	–	6.3	5.3	5.9	5.6	5.7	5.6
	d_{90}	10.8	–	8.4	7.9	7.8	8.1	7.6	7.8
	d_{80}	11.6	–	10.2	8.8	9.3	8.4	8.3	8.4
12 MeV		LMA	STR thickness (mm)						
			2.0	4.0	6.0	8.0	10.0	12.0	14.0
	Surface	3.0	–	–	0.7	0.5	1.0	0.6	0.5
	d_{max}	9.3	–	9.8	9.3	9.3	9.2	10.0	9.8
	d_{90}	14.7	–	15.0	13.2	15.9	14.7	15.3	16.6
	d_{80}	18.4	–	16.9	15.5	16.8	16.6	17.5	18.6

using the LMA, the corresponding values were 5.7 and 3.0 mm, 9.7 and 9.3 mm, 10.8 and 14.7 mm, and 11.6 and 18.4 mm, respectively. Corresponding $P_{80\text{-}20}$ values could not be obtained with STR thickness 1.0, 2.0, and 4.0 mm because these STR thicknesses could not shield > 80% of the dose.

3.3. Comparison of transmission rates between measurement and calculation against γ-rays from ^{192}Ir

Fig. 7 shows the measured and simulated transmission rates of the STR and thickness ranging from 1.0 mm to 16.0 mm. The STR thickness that obtained a 50% reduction rate for ^{192}Ir was 5.804 mm. In contrast, the corresponding value for lead with ^{192}Ir is 5.8 mm [28]. The Monte Carlo calculation results were 2.6% higher on average than the measured results, whereas normally, experimental measurements and Monte Carlo calculation results have been similar. The differences between Monte Carlo calculations and measurements at each STR thickness ranged from 1.36% to 3.95%. The average standard error was 2.49%.

4. Discussion

We have developed a novel real time STR that can be changed shape by hand at a temperature of approximately 60 °C and maintains its shape at room and body temperatures. In this study, we investigated the STR's viscoelasticity and usability for electron therapy and brachytherapy. The STR's density is an important factor because of the tradeoff relationship between viscoelasticity and shielding ability. A density value of 7.3 g/cm^3 is suitable for clinical use because the following characteristics of viscoelasticity are preferable: 1. Elastic behavior in the body temperature region to maintain the STR's shape as a shielding material, 2. Viscosity at high temperatures (e.g., 60 °C) for

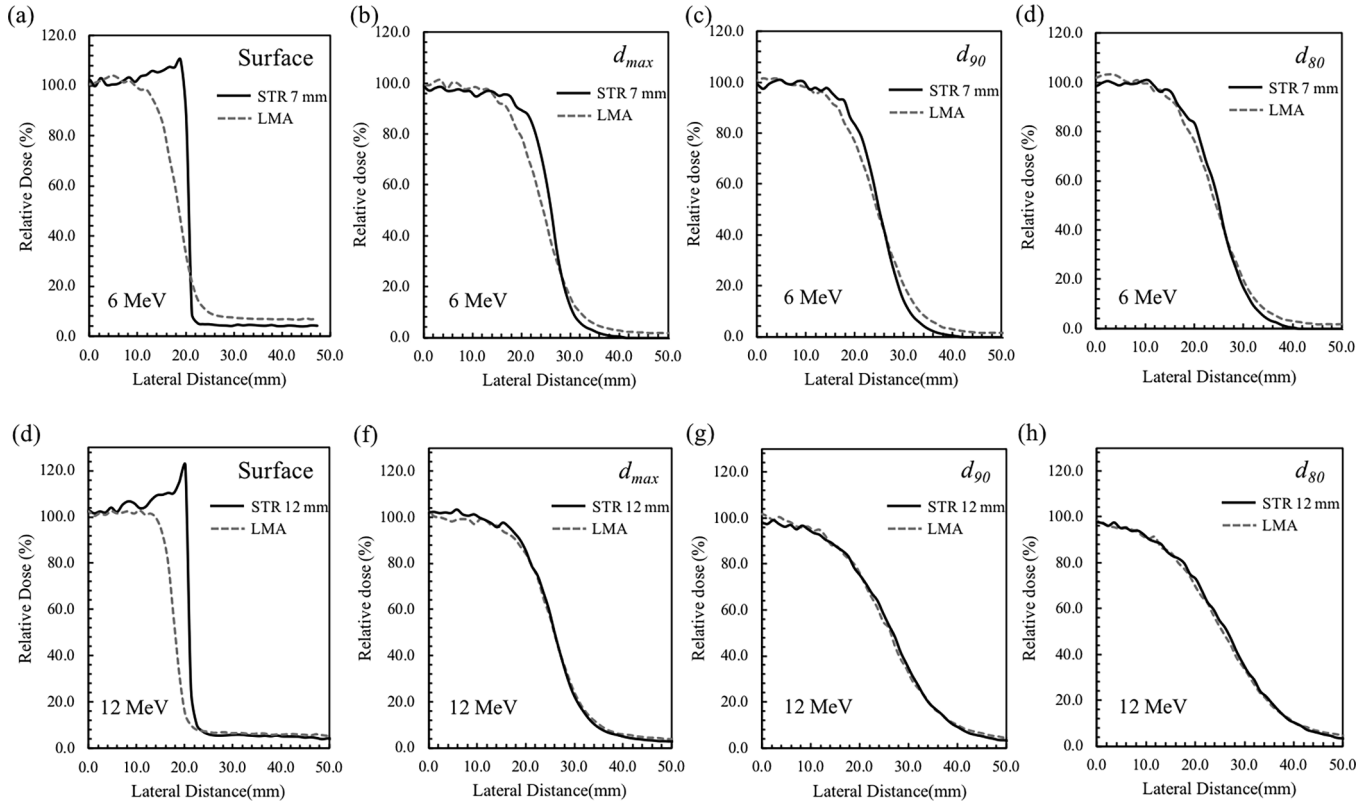

Fig. 6. Lateral dose profiles at surface, d_{max}, d_{90}, and d_{80} for LMA and STR with thickness of 7.0 and 12.0 mm for 6 and 12 MeV electron beams.

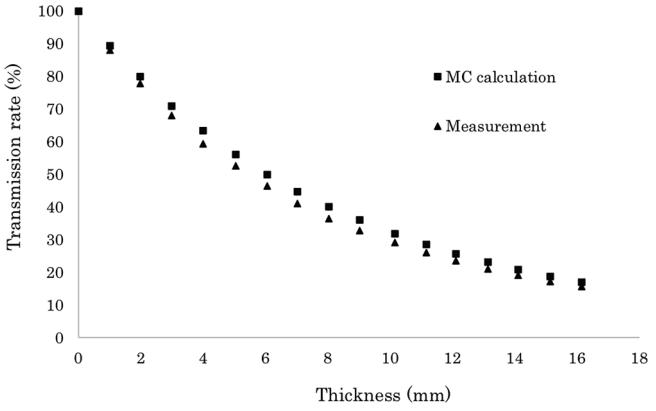

Fig. 7. Comparison of transmission rate between Monte Carlo calculation and measurement with ^{192}Ir source and STR thickness of 0.0 (air) to 16.0 mm.

easy real-time processing and variable shaping, 3. Adequate shielding ability against megavoltage electron beams and γ-rays from ^{192}Ir, even with low thickness. In addition, the STR can be used permanently, while maintaining the quality of shielding-effect. However, it shall not be applied when the STR is contaminated by blood and body fluids.

In electron radiotherapy, the STR is easy to shape and place on a curved part of a patient's body, such as the face, ear, shoulder, or belly. The STR can suppress the target's movements, including respiration and patient motion, which can also reduce the extra margin. In addition, the STR may be applied in intraoperative electron radiotherapy [7,29]. The transmission rates with STR thickness of 1.0 and 2.0 mm were higher than those without STR for 6 and 12 MeV electron beams because the interaction between the STR and the electron beams caused bremsstrahlung [30]. Except for those conditions, the transmission rate decreased exponentially with increased STR thickness, and these findings correlated well with those of previous studies [4,11]. The PDD results shown in Table 3 and Fig. 5 illustrate that the d_{max}, d_{90}, *and* d_{80} values were almost equal between LMA for all thickness values of STR; therefore, the PDD values were not significantly influenced by shielding effects of the LMA or STR. The maximum doses at d_{max}, d_{90}, and d_{80} were similar between LMA and STR. However, the maximum dose at the surface using STR was increased compared with that of LMA due to differences of shielding position, bremsstrahlung, penetration, and lateral ray scattering [11]. However, the relative magnitudes of those high doses were approximately 80% and 90% for 6 and 12 MeV electron beams because the PDD values at the surface were approximately 60%–70% as shown in Fig. 5.

The transmission rates of STRs against γ-rays from ^{192}Ir at room temperature reduced exponentially with increasing thickness in the range from 0.0 mm to 16.0 mm. An STR thickness of 5.8 mm shielded approximately 50% of the dose and has high shielding ability, demonstrating the possibility of clinical application. In addition, both measurements and calculations were adequately accurate, as the dose difference between simulation and measurement was within 4.0%, a smaller value than the corresponding one obtained in another report (i.e., about 5.6%, described by Shi et al. [31]).

There are three widely accepted principles for reducing radiation exposure: time, distance, and shielding. Therefore, several previously developed techniques have focused on the distance from the source to normal tissue and shielding to prevent severe complications such as mucositis and osteonecrosis from HDR brachytherapy [23,32]. Obinata et al. showed that the use of a thicker spacer (i.e., ≥10 mm) could minimize the risk of osteoradionecrosis from 18.2% (< 5 mm) to 0% (≥5 mm) in patients who received LDR brachytherapy for tongue cancer [33]. Their data seem reasonable because greater radiation doses should be absorbed by thicker spacers [23]. However, the limited space between the tongue and mandible might make placing a spacer challenging [34]. Murakami et al. described that oral devices containing lead successfully increased the distance and shielding from the source [23]. Adding lead apparently decreased the absorbed dose even

if the distance to the source was short. STR has several advantages over lead-containing oral devices in a clinical practice. STR can be flexibly modified in terms of the shape and thickness. In addition, STR is a safer material than lead. Based on the results in this study, STR could be useful to overcome problems associated with devices containing lead.

We have described a novel lead-free radiation-shielding material, STR, and characterized its radiation shielding ability against electron beams and pre- and post-operative radiation protection in brachytherapy [5,35] within the energy range used in radiotherapy. STR has potential applications as a radiation-shielding material and has several benefits, including being easy to shape in real time, reusable, and ecofriendly. This new STR is lead-free and has many unique features that could be useful for both indoor and outdoor industrial use.

5. Conclusion

STR can be changed shape by hand at approximately 60 °C and maintains its shape under room and body temperatures. It has adequate radiation shielding ability against electrons in the energy range used in radiotherapy and brachytherapy with ^{192}Ir. Therefore, it can be employed instead of lead and has the potential to open a new era of radiation protection.

Acknowledgments

This work was supported partly by Japan Society for the Promotion of Science (JSPS) KAKENHI grant number 19K08211. We thank Mr. Masafumi Shigita and Mr. Yoshito Kadowaki for their support. We thank Richard Lipkin, PhD, from Edanz Group (www.edanzediting.com/ac) for editing a draft of this manuscript.

Declaration of Competing Interest

Hajjme Monzen received a research donation from Hayakawa Rubber Co., Ltd.

References

[1] Rempel D. The lead-exposed. JAMA 1989;262:5.
[2] Rizescu C, Cirstea E. Lead poisoning. Metal Int 2008;13:56–61. https://doi.org/10.1146/annurev.med.55.091902.103653.
[3] Peuster M, Fink C, Von Schnakenburg C. Biocompatibility of corroding tungsten coils: In vitro assessment of degradation kinetics and cytotoxicity on human cells. Biomaterials 2003;24:4057–61. https://doi.org/10.1016/S0142-9612(03)00274-6.
[4] Fujimoto T, Monzen H, Nakata M, Okada T, Yano S, Takakura T, et al. Dosimetric shield evaluation with tungsten sheet in 4, 6, and 9MeV electron beams. Phys Med 2014;30:838–42. https://doi.org/10.1016/j.ejmp.2014.05.009.
[5] Inada M, Monzen H, Matsumoto K, Tamura M, Minami T, Nakamatsu K, et al. A novel radiation-shielding undergarment using tungsten functional paper for patients with permanent prostate brachytherapy. J Radiat Res 2018;59:333–7. https://doi.org/10.1093/jrr/rry030.
[6] Monzen H, Kanno I, Fujimoto T, Hiraoka M. Estimation of the shielding ability of a tungsten functional paper for diagnostic x-rays and gamma rays. J Appl Clin Med Phys 2017;18:1–5. https://doi.org/10.1002/acm2.12122.
[7] Kamomae T, Monzen H, Kawamura M, Okudaira K, Nakaya T, Mukoyama T, et al. Dosimetric feasibility of using tungsten-based functional paper for flexible chest wall protectors in intraoperative electron radiotherapy for breast cancer. Phys Med Biol 2017;63:015006https://doi.org/10.1088/1361-6560/aa96cf.
[8] Monzen H, Tamura M, Shimomura K, Onishi Y, Nakayama S, Fujimoto T, et al. A novel radiation protection device based on tungsten functional paper for application in interventional radiology. J Appl Clin Med Phys 2017;18:215–20. https://doi.org/10.1002/acm2.12083.
[9] Tamura M, Monzen H, Kubo K, Hirata M, Nishimura Y. Feasibility of tungsten functional paper in electron grid therapy: a Monte Carlo study. Phys Med Biol 2017;62:878–89. https://doi.org/10.1088/1361-6560/62/3/878.
[10] Kawai Y, Tamura M, Amano M, Kamomae T, Monzen H. Dosimetric characterization of a novel surface collimator with tungsten functional paper for electron therapy. Anticancer Res 2019;39:2839–43. https://doi.org/10.21873/anticanres.13412.
[11] Kijima K, Monzen H, Matsumoto K, Tamura M, Nishimura Y. The shielding ability of novel tungsten rubber against the electron beam for clinical use in radiation therapy. Anticancer Res 2018;38:3919–27. https://doi.org/10.21873/anticanres.12677.
[12] Kosaka H, Monzen H, Matsumoto K, Tamura M, Nishimura Y. Reduction of operator hand exposure in interventional radiology with a novel finger sack using tungsten-containing rubber. Health Phys 2019;116:625–30. https://doi.org/10.1097/HP.0000000000000992.
[13] Kijima K, Krisanachinda A, Tamura M, Nishimura Y, Monzen H. Feasibility of a tungsten rubber grid collimator for electron grid therapy. Anticancer Res 2019;39:2799–804. https://doi.org/10.21873/anticanres.13407.
[14] Prasad SG, Parthasaradhi K, Lee Y, Garces R. Lead shielding thickness for dose reduction of 5 MeV electrons. Med Phys 1989. https://doi.org/10.1118/1.596432.
[15] Khan FM, Moore VCLS. Field shaping in electron beam therapy. Br J Radiol 1976;49:883–6. https://doi.org/10.1259/0007-1285-49-586-883.
[16] Khan FM, Werner BL, Deibel FC. Lead shielding for electrons. Med Phys 1981;8:712–3. https://doi.org/10.1118/1.594841.
[17] Ospedaliero A, Policlinico U, Emanuale V. Potential exposure to carcinogens in low-melting alloys processingle. G Ital Med Lav Erg 2013;35:73–6.
[18] Van Leeuwen MCE, Stokmans SC, Bulstra AEJ, Meijer OWM, Heymans MW, Ket JCF, et al. Surgical excision with adjuvant irradiation for treatment of keloid scars: a systematic review. Plast Reconstr Surg Glob Open 2015;3:e440https://doi.org/10.1097/GOX.0000000000000357.
[19] Skowronek J. Current status of brachytherapy in cancer treatment – short overview. J Contemp Brachytherapy 2017;9:581–9. https://doi.org/10.5114/jcb.2017.72607.
[20] Yamazaki H, Yoshida K, Yoshioka Y, Shimizutani K, Furukawa S, Koizumi M, et al. High dose rate brachytherapy for oral cancer. J Radiat Res 2013;54:1–17. https://doi.org/10.1093/jrr/rrs103.
[21] Akiyama H, Yoshida K, Shimizutani K, Yamazaki H, Koizumi M, Yoshioka Y, et al. Dose reduction trial from 60 Gy in 10 fractions to 54 Gy in 9 fractions schedule in high-dose-rate interstitial brachytherapy for early oral tongue cancer. J Radiat Res 2012;53:722–6. https://doi.org/10.1093/jrr/rrs027.
[22] Yoshida K, Takenaka T, Akiyama H, Yamazaki H, Yoshida M, Masui K, et al. Three-dimensional image-based high-dose-rate interstitial brachytherapy for mobile tongue cancer. J Radiat Res 2014;55:154–61. https://doi.org/10.1093/jrr/rrt079.
[23] Murakami S, Verdonschot RG, Kakimoto N, Sumida I, Fujiwara M, Ogawa K, et al. Preventing complications from high-dose rate brachytherapy when treating mobile tongue cancer via the application of a modular lead-lined spacer. PLoS ONE 2016;11:e0154226https://doi.org/10.1371/journal.pone.0154226.
[24] Jung JY, Lu B, Yoon DK, Hong KJ, Jang HS, Liu C, et al. Therapy region monitoring based on PET using 478 keV single prompt gamma ray during BNCT: a Monte Carlo simulation study. Phys Med 2016;32:562–7. https://doi.org/10.1016/j.ejmp.2016.02.010.
[25] Geethamma VG, Kalaprasad G, Groeninckx G, Thomas S. Dynamic mechanical behavior of short coir fiber reinforced natural rubber composites. Compos Part A Appl Sci Manuf 2005;36:1499–506. https://doi.org/10.1016/j.compositesa.2005.03.004.
[26] Najib NN, Ariff ZM, Bakar AA, Sipaut CS. Correlation between the acoustic and dynamic mechanical properties of natural rubber foam: effect of foaming temperature. Mater Des 2011;32:505–11. https://doi.org/10.1016/j.matdes.2010.08.030.
[27] Ivanova KI, Pethrick RA, Affrossman S. Investigation of hydrothermal ageing of a filled rubber toughened epoxy resin using dynamic mechanical thermal analysis and dielectric spectroscopy. Polymer 2000;41:6787–96. https://doi.org/10.1016/S0032-3861(00)00042-2.
[28] Papagiannis P, Baltas D, Granero D, Gimeno J, Ballester F, Venselaar JLM. Radiation transmission data for radionuclides and materials relevant to brachytherapy facility shielding. Med Phys 2008;35:4898–906. https://doi.org/10.1118/1.2986153.
[29] Alhamada H, Simon S, Philippson C, Vandekerkhove C, Jourani Y, Pauly N, et al. Shielding disk position in intra-operative electron radiotherapy (IOERT): a Monte Carlo study. Phys Med 2018;51:1–6. https://doi.org/10.1016/j.ejmp.2018.05.023.
[30] Podogorsak EB. Radiation oncology physics: a handbook for teachers and students. Int At Energy Agency 2005. https://doi.org/10.1021/jf030837o.
[31] Shi C, Wang B. Preliminary Monte Carlo investigation of using Ir-192 as the source for real time imaging purpose. Int J Med Phys Clin Eng Radiat Oncol 2017;6:21–30. https://doi.org/10.4236/ijmpcero.2017.61003.
[32] Kudoh T, Ikushima H, Kudoh K, Tokuyama R, Osaki K, Furutani S, et al. High-dose-rate brachytherapy for patients with maxillary gingival carcinoma using a novel customized intraoral mold technique. Oral Surgery Oral Med Oral Pathol Oral Radiol Endod 2010;109:e102–8. https://doi.org/10.1016/j.tripleo.2009.10.019.
[33] Obinata K, Ohmori K, Tuchiya K, Nishioka T, Shirato H, Nakamura M. Clinical study of a spacer to help prevent osteoradionecrosis resulting from brachytherapy for tongue cancer. Oral Surg Oral Med Oral Pathol Oral Radiol Endod 2003;95:246–50. https://doi.org/10.1067/moe.2003.94.
[34] Kakimoto N, Inoue T, Inoue T, Murakami S, Furukawa S, Yoshida K, et al. Results of low- and high-dose-rate interstitial brachytherapy for T3 mobile tongue cancer. Radiother Oncol 2003;68:123–8. https://doi.org/10.1016/S0167-8140(03)00055-0.
[35] Busoni S, Fedeli L, Belli G, Genovese E, Cannatà V, Gori C, et al. Pre and post operative radiation protection in Ru-106 brachytherapy ophthalmic plaque surgery and related material shielding properties. Phys Med 2019;57:245–50. https://doi.org/10.1016/j.ejmp.2018.11.003.